Available online www.ejaet.com

European Journal of Advances in Engineering and Technology, 2020, 7(4):16-22

Research Article ISSN: 2394 - 658X

Study of Physical and Chemical Properties on Modified Smectite Catalysts Using HDTMA Cation

Shu-Lung Kuo and Ching-Lin Ho*

Department of Technology Management, Open University of Kaohsiung, Taiwan
**Email: hcl6005@ouk.edu.tw*

ABSTRACT

This study used commercially available smectite as the catalyst carrier and modified it with hexadecyl trimethyl ammonium cation (HDTMA) through ion exchange, forming nano-level HDTMA-modified smectite via surface modification and high-temperature sintering. The physical and chemical properties of the smectite and the HDTMA-modified smectite were then studiedthrough a series of physical and chemical experiments, such as specific surface area analysis, Fourier-transfer infrared spectrometer (FT-IR) analysis, X-ray diffraction (XRD) analysis, field emission scanning electron microscope (FE-SEM) analysis, and potentiometric titration analysis.

First, the modified smectite had a larger specific surface area than the HDTMA-modified smectite that had undergone ion exchange, suggesting that the OH groups on the surface of the HDTMA-modified smectite reacted with each other and produced condensed bonds when sintered at high temperature, causing the specific surface area to decline. In terms of the FT-IR analysis, the result showed that -CH_2- and -CH_3- absorption bonds increased at multiple wavenumber positions, signifying that methyl molecules or carbon and hydrogen atoms in the alkyl carbon chain were successfully inserted into the smectite. As for the XRD analysis, we found that water molecules could easily enter the smectite interlayers because the X-crystal lattices of the smectite were susceptible to the humidity of the environment. Also, the smectite showed significant expansion and contraction after being steamed with glycerol.On the other hand, the FE-SEM analysis showed that the modified smectite surface attracted a large amount of crystalized HDTMA after ion exchange and sintering at 350°C, creating an irregular shape; however, the modified smectite was still able to maintain the loose and cotton flake-like structure of the ordinary smectite. Finally, the potentiometric titration analysis suggests that the equivalence point of the HDTMA-modified smectite on the titration curve was not noticeable, and the change of the curve was divided into two phases; this means that the HDTMA-modified smectite contained more acidic functional groups than the smectite did.

Key words: HDTMA, smectite catalyst, XRD, FE-SEM

---

1. INTRODUCTION

Photocatalysis has been demonstrated as an unique and efficient process for decomposing organic pollutants by the utilization of solar energy, where the bandgap of semiconductor plays a vital role in the generation of photo-induced electron–hole pairs [1]. As the photo-degradation efficiency strongly depends on the electron–hole pair utilization, the recombination of these pairs in a semiconductor can influence the decomposing process of organic pollutants [2]. Since the photocatalysis embarked, anatase TiO_2 is demonstrated as an efficient photocatalyst (bandgap of 3.0–3.2 eV) due to its great hole trapping ability and photochemical stability [3-4]. In recent years, bismuth-based catalysts have been revealed enhanced efficiencies over than that of TiO_2, due to their intrinsic property of layered structure with the presence of electrostatic forces between anions and cations [5-6]. Though BiOCl exhibits its excellence in the superior degradation activity, due to the large bandgap (3.4–3.6 eV), there is still degradation limitation for BiOCl and to avoid this, researchers fabricated BiOClheterostructures to realize higher efficiency [7].

In recent years, another efficient way to improve the kinetics of photocatalyses is the addition of transition metals such as silver (Ag^+) to the TiO_2 catalyst [8-9]. Nano-scale silver clusters release atomic Ag(0) that is as effective as chemical species Ag(I) ions to rapidly kill bacteria and fungi. Besides, the nano-scale silver-doped TiO_2 photocatalyses (nano-Ag/TiO_2) particles have attracted much interest due to their antibacterial and biomedical applications [10-11]. Although there is extensive literature on the use of Ag^+ ion doped TiO_2 for photocatalytic degradation of organics, its application

for photocatalytic disinfection of indoor air with bacterial pollutions has not been fully studied (Shie et al., 2008), especially for on-site indoor air disinfection for our living environment such as museum, nursing institutions, schools, and other public areas.

This study explored the physical and chemical properties of HDTMA-modified smectite and ways to analyze such properties through the application of different instruments. The commercially available smectite was used as the primary catalyst carrier and modified with HDTMA through ion exchange, forming the so-called HDTMA-modified smectite. The results of these analyses can be applied to catalytic reactions for a wide range of pollutants.

2. MATERIALS AND METHODS

2.1. Purification and preparation of sodium saturated smectite

Put 60 g commercially available smectite into a 2-liter beaker, and add 1.8 liters of deionized water to it. After stirring, soak it for days to fully expand it. After it is expanded, take 250 ml of the smectite suspension out of the beaker. Filter sand using the wet sieving method with a 300-mesh sieve. Transfer the filtrate to a 1-liter sedimentation cylinder, and add deionized water to make 1 liter. Leave it to naturally sediment after stirring it rigorously with a stirring rod. Siphon the suspension at the top of the sedimentation cylinder by 10 cm 8 hours later. Use an 18000 rpm high-speed centrifuge to have the suspension centrifuged. Perform sodium saturation of the smectite obtained after centrifugation with 1 M NaCl solution. Next, grind the saturated smectite into powder with an agate mortar after freeze drying it, and obtain the sodium saturated smectite.

2.2. Resource and identification of HDTMA

The HDTMA used in this study was mainly purchased from Lancaster Synthesis. HDTMA mostly functions as a non-ionic surfactant for industrial use. Its molecular formula is $C_{16}H_{33}(CH_3)_3NBr$, and its molecular weight is 364.46 g/mol.

2.3. Preparation of smectite-HDTMA

Take 0.5 g sodium saturated smectite and add 30 ml of the HDTMA solution with a value equivalent to 0.75 times the CEC value. Continuously heat it up and oscillate it in a water bath at 80^{o}C for 24 h. Separate a solid from the liquid using a high-speed centrifuge at 20,000 rpm. Inspect whether the supernatant has white sediment after centrifugation using $AgNO_3$, to ensure that the chloride ions have been completely removed. After freeze-drying the modified smectite-HDTMA, grind it using an agate mortar and then store it. Conduct the subsequent characteristic analysis and absorption test.

2.4. Analysis of the properties of smectite-HDTMA

2.4.1. Verification of the function group of fourier-transform infrared spectroscopy (FT-IR)

The principle of FT-IR is using rotations or vibrations of molecules to absorb radiation at the same frequency. The fingerprint and Eigen areas in FT-IR can help to determine the existence of isomorphous replacement structure or organic molecules in the smectite and smectite-HDTMA.

Put the smectite and smectite-HDTMA and KBr powders in an oven. After heating them up and drying them for 48 hours, mix them evenly in a 1:10 ratio, and then grind the mixture with an agate mortar. Use a hydraulic press to press the mixture at 10 tons/hour, making it into a transparent foil. Put the foil in a spectrometer and perform an analysis with a scan range of 4,000 cm^{-1} to 400 cm^{-1}.

2.4.2. X-ray Diffraction Analysis (XRD Analysis)

The XRD analysis is conducted using an x-ray diffractometer (Rigaku RINT-2000). With CuK_a as the light source, an analysis on the crystal patterns of the smectite and smectite-HDTMA is performed to learn the spacing of layers of materials. The x-ray wavelength produced is 1.5418 Å; the operating current during testing is 10 mA; the voltage is 20 kV; the scanning speed is 5 deg/min; and the scanning angle is $2\theta=2\sim40^{o}$.

2.4.3. Specific surface area measurement

This study adopted ethylene glycol tests to measure the total specific surface area of the smectite and HDTMA-modified smectite.

$$A = \frac{W_a}{(W_S \times K)}$$

A: specific surface area (m^2/g);

W_a: The value of weight change before and after absorbing ethylene glycol (g)

W_s: weight before absorbing ethylene glycol (g); K: 0.00031

2.5. Fieldemission scanning electron microscope (FE-SEM) analysis of smectite-HDTMA

With a scanning electron microscope (SEM), this study observes the properties of smectite and smectite-HDTMA and their distribution. The model in use is JEOL-6330, and its emitting energycomes from the field emission filament with high space and energy resolution.

2.6. Potentiometric titration analysis

Potentiometric titration primarily uses changes in the electrode potentials of solutions to represent changes in titration curves. It also uses changes in pH values to observe the properties of acidic function groups. The steps for the experiment are as follows: 0.3 g smectite and smectite-HDTMA are put into a beaker, respectively, and 300 mL of deionized water are added. Acidify 0.1 M HNO_3 to pH 3. Add 0.2 mL of a 0.1 M concentration of NaOH solution each time to perform the titration. Changes in pH values and electric potentials are recorded after approximately 5 minutes when the titration is stabilized; recording is continued until reaching pH11.

3. RESULTS AND DISCUSSION

3.1. The measurement of specific areas of smectite and HDTMA-modified smectite

In this study, we used ethylene glycol tests to measure the specific surface areas of the smectite and HDTMA-modified smectite; the results are shown in Table 3-1. From Table 3-1, we know that the smectite has a larger specific surface area compared with the HDTMA-modified smectite that had undergone ion exchange. The specific surface area of the smectite was 545 m^2/g, while that of the HDTMA-modified smectite was 458 m^2/g. We assume the main reason causing the specific surface area of the HDTMA-modified smectite to shrink is that the •OH groups on its surface reacted with each other, triggering condensing reactions, nucleation, and crystallization.

Table -1 The specific surface areas of the smectite and HDTMA-modified smectite

Type	Scpcific surface area
	----------m^2/g----------
smectite	545
smectite-HDTMA	458

3.2. Results of FT-IR analysis with HDTMA and smectite-HDTMA

Figures 1(a)-(c) indicate the results of the FT-IR analyses on HDTMA, smectite and HDTMA-modified smectite, respectively. Figure 1(b) shows many distinctive and complex peaks inside the fingerprint region between 750~1170 cm^{-1}, which reflects the existence of impure silicate (Si-O) and silicate (O-Si-O) bonds in silicate minerals. The -OH on the metal ion layer (octahedral layer) bends and vibrates, resulting in different absorption properties because Al^{+3} partially replaced Si^{+4} in the silicate layer (tetrahedral layer), and many metal ions could enter the octahedral layer. Besides, from Figure 1(b), we can see that absorption peaks of octahedral -OH on the smectite only occur at wavenumber between 3400-3700 cm^{-1}, but after being modified with HDTMA, the absorption peaks of $-CH_2-$ and $-CH_3$ appear at 2910, 2846, and 1461 cm^{-1}; this suggests that methyl molecules or carbon and hydrogen atoms in the alkyl carbon chain were successfully inserted into the structure of the smectite [12]. The results prove that HDTMA-modified smectite should have enough capacity to degrade pollutants during catalytic reactions.

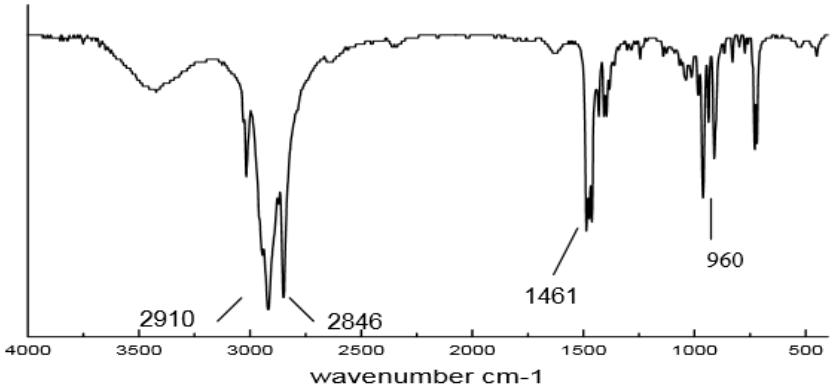

(a) HDTMA

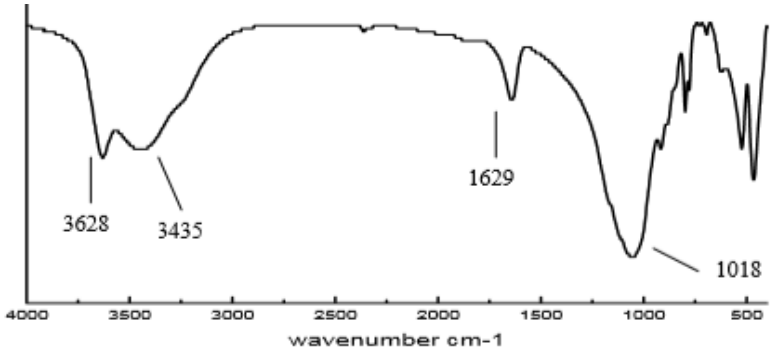

(b) smectite

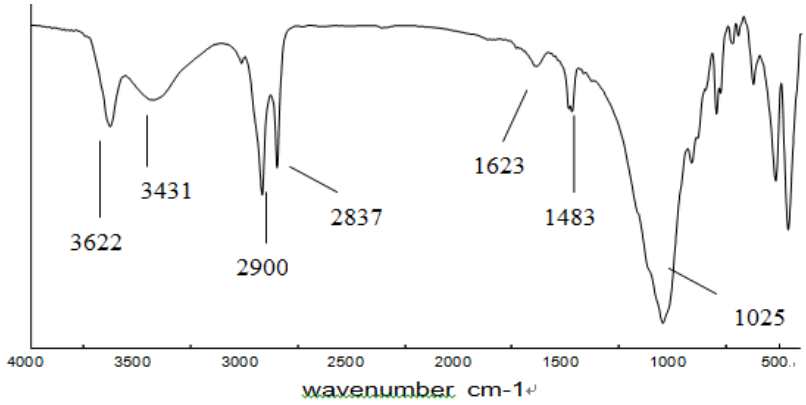

(c) smectite-HDTMA

Fig. 1 FT-IR spectrum of HDTMA, smectite and smectite-HDTMA

3.3 Results of XRD analysis

3.3.1 Results of smectite XRD analysis

The XDR analysis on the smectite clay presents noticeable diffraction peaks after the purification and saturation processes using potassium and magnesium. The X-crystallattices of the smectite are susceptible to the humidity of the atmosphere, allowing water molecules easy entry into its interlayers. After saturating it with magnesium and steaming it with glycerol, the interlayers of the smectite clay expanded [13]. On the other hand, after saturating the clay with potassium and heating it, the interlayers contracted due to moisture loss. From Figure 2, we know that the diffraction peak of the potassium-saturated smectite at room temperature is 1.229 nm. When heated to 110°C, 350°C, and 550°C, thespacing of layers of the potassium-saturated smectite declined to 1.155nm, 1.017nm, and 1.004 nm, respectively. In contrast, that of the magnesium-saturated smectite at room temperature increased from 1.551 nm to 1.846 nm after being steamed with glycerol. From the XDR graph below, we can see that the contraction and expansion of the smectite are relatively remarkable.

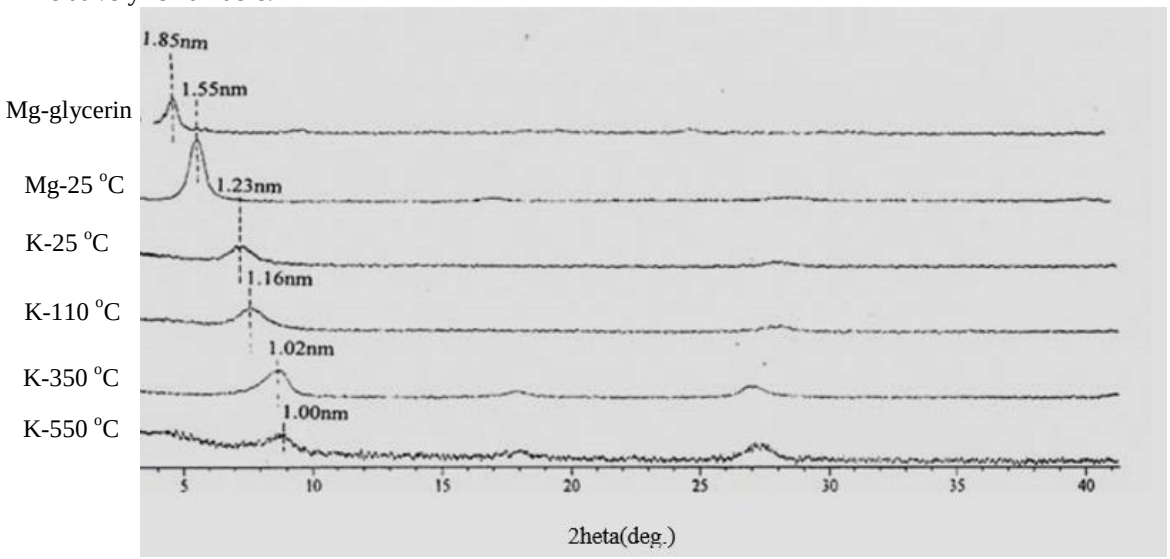

Fig. 2 XRD analysis of smectite

3.3.2. Results of smectite-HDTMA XRD analysis

Figure 3 shows the observation on the changes in the spacing of layers before and after modifying the smectite clay with HDTMA. The results indicate that the spacing of the layers was 1.05nm before the smectite was modified with HDTMA; the spacing of the layers increased 0.63nm to 1.68 nm after the clay was modified with HDTMA. The results suggest that alkyl ammonium was inserted into the interlayers of the smectite clay and formed a double-layered alkyl ammonium structure, indicating that the application of the HDTMA-modified smectite as catalysts was feasible and that the modified smectite can facilitate the electronic transition in the clay [14].

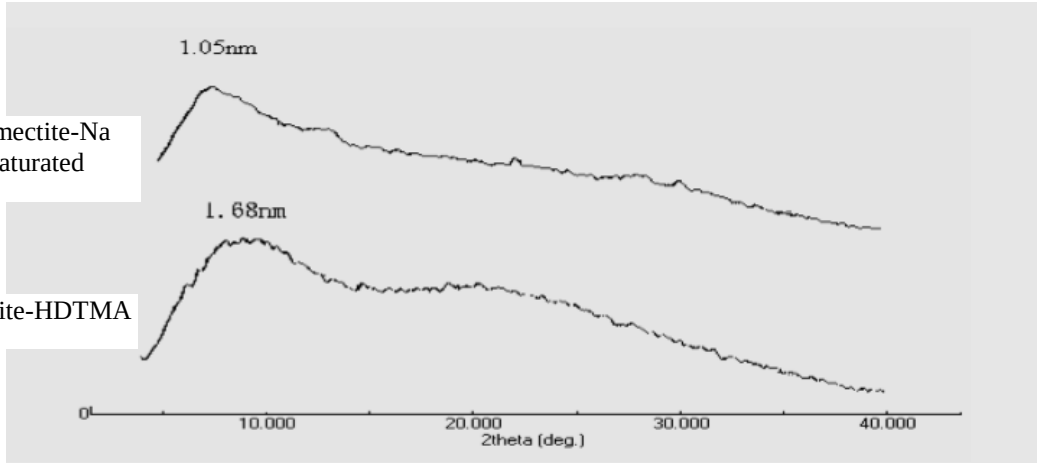

Fig. 3 XRD analysis of Na-saturated smectite and scmectite-HDTMA

3.4. Results of FE-SEM analysis of smectite and smectite-HDTMA

Figures 4 and 5 demonstrate the surface structure of the smectite and HDTMA-modified smectite observed through an SEM-EDS analysis, respectively. Figure 4 shows that the smectite is characterized by a loose, cotton flake-like, or layered structure because it is a kind of expansive clay. Figure 5 presents the analysis of the smectite that was modified by HDTMA through ion exchange and sintered at 350°C. We can see a significant amount of crystalized HDTMA sticking to the surface of the modified smectite, creating an irregular shape [14]. However, the HDTMA-modified smectite still maintained the loose and cotton flake-like structure of the ordinary smectite.

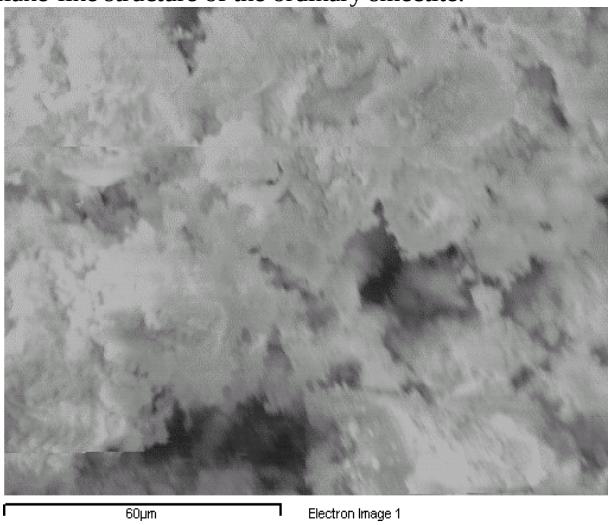

Fig. 4 FE-SEM analysis of smectite (100,000x magnification)

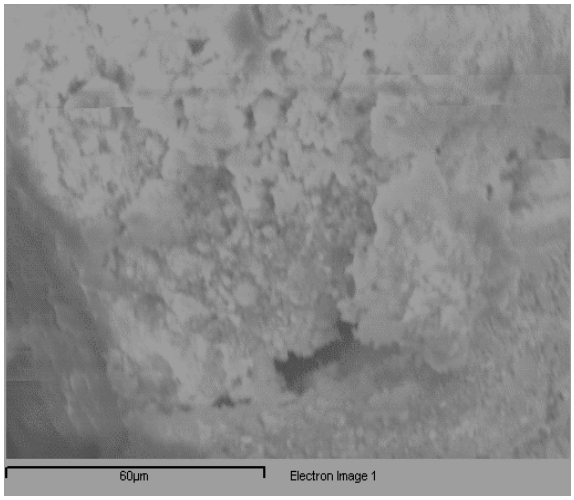

Fig. 5 FE-SEM analysis of HDTMA-modified smectite (100,000x magnification)

3.5. Results of potentiometric titration analysis of smectite and smectite-HDTMA

Figure 6 shows the potentiometric titration curve of the smectite and HDTMA-modified smectite. As shown in the figure, there is a drastic change in the pH value of the smectite when it was closer to the equivalence point. On the other hand, the titration curve of the HDTMA-modified smectite was less curvy and had two equivalence points, signifyingthat the change in the pH value was divided into two phases; this also indicates that the HDTMA-modified smectite underwent two phases of dissociation during titration. Furthermore, we can see from the graph that the pH value of the smectite when it reached the equivalence point was 7, suggesting that it was neutral. The titration endpoint appeared when the amount of added NaOH reached 5 mL. The endpoint of the HDTMA-modified smectite titration appeared when the amount of added NaOH reached 7mL.

Figure 7 is a function obtained by differentiating the potentiometric potential caused by NaOH per unit; the maximum is the endpoint of the titration (equivalence point). As shown in the figure, there is only one endpoint in the smectite titration, while there are two in the HDTMA-modified smectite titration, suggesting that the HDTMA-modified smectite contained two different acidic functional groups. The results prove that the HDTMA-modified smectite had more acidic functional groups than the smectitedid [15] when the smectite was undergoing ionic or molecular modification. For instance, Figure 7 shows that the HDTMA-modified smectite has two considerably noticeable acidic functional groups, echoing the findings of Figure 6, in which there are two phases of disassociation of the HDTMA-modified smectite during titration.

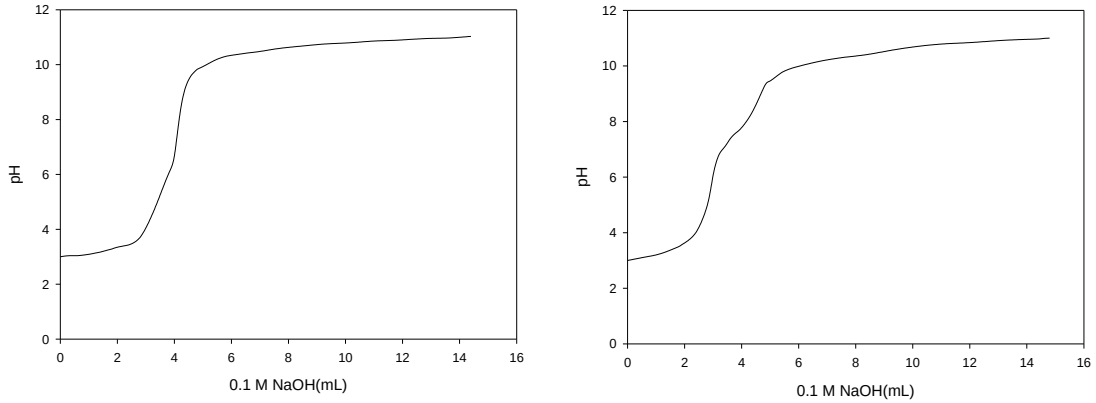

(a) smectite (b) smectite-HDTMA

Fig. 6 Titration curves of smectite and HDTMA-modified smectite

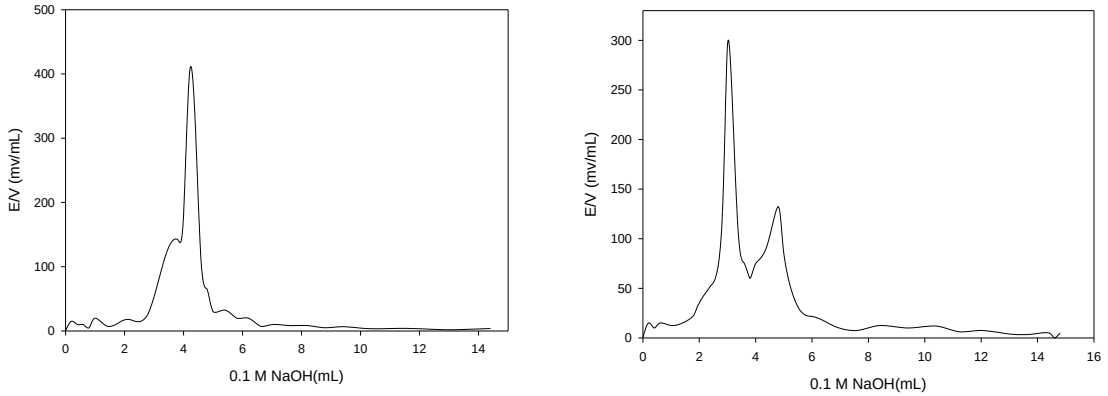

(a) smectite (b) smectite-HDTMA

Fig. 7 Differentiated titration curves of smectite and HDTMA-modified smectite

4. CONCLUSION

This study adopted smectite clay as the catalyst carrier and modified the clay surface with HDTMA through ion exchange. It then explored the physical properties of the HDTMA-modified smectite via various instruments and physical and chemical experiments. In terms of the analysis of the specific surface area of the clay, we found that the specific surface area of the smectite (545 m^2/g) is larger than that of the HDTMA-modified smectite (458 m^2/g) because the •OH groups on the surface of the modified clay reacted with each other, forming condensed bonds and triggering nucleation and crystallization, which caused the specific surface area to shrink. In terms of the FT-IR analysis, $-CH_2-$ and $-CH_3$

absorption peaks occurred at wavenumber 2910, 2846, and 1461 cm^{-1}, suggesting that methyl molecules or the carbon and hydrogen atoms in the alkyl carbon chain were successfully inserted into the structure of the smectite clay. In terms of the XDR analysis, we discovered that thespacing of layers of the smectite expanded after it was modified by HDTMA, indicating that alkyl ammonium was inserted into the interlayers of the clay and formed a double-layered alkyl ammonium structure. Finally, the results of the potentiometric titration analysis show that there are two equivalence points in the titration curve of the HDTMA-modified smectite, signifying that the HDTMA-modified smectite contains more acidic functional groups than its unmodified counterpart. These findings suggest that the HDTMA-modified smectite should have enough functional groups to absorb and degrade pollutants in catalytic reactions.

REFERENCES

[1]. Yamashita, H., Harada, M., Tanii, A., (2000). Preparation of efficient titanium oxide photocatalysts by an ionized cluster beam (ICB) method and their photocatalytic reactivities for the purification of water. Catalysis Today 63, 63-69.

[2]. Konstantinou, I.K., Albanis, T.A., 2004. TiO_2-assisted photocatalytic degradation of azo dyes in aqueous solution: kinetic and mechanistic investigations. Applied Catalysis B: Environmental 49, 1-14.

[3]. Zhang, Z., Wang, W., Shang, M., 2010. Low-temperature combustion synthesis of Bi2WO6 nanoparticles as a visible-light-driven photocatalyst. Journal of Hazardous Materials177, 1013-1018.

[4]. Naeem, K., Ouyang, F., 2010. Preparation of Fe^{3+}-doped TiO_2 nanoparticles and its photocatalytic activity under UV light. Physica B405, 221-226.

[5]. Gao, X., Zhang, X., Wang, Y., 2015. Rapid synthesis of hierarchical BiOCl microspheres for efficient photocatalytic degradation of carbamazepine under simulated solar irradiation. Chemical Engineering Journal 263, 419-426.

[6]. Li, X., Zhu, C., Song, Y., 2017. Solvent co-mediated synthesis of ultrathin BiOCl nanosheets with highly efficient visible-light photocatalytic activity. RSC Advances 7, 10235-10241.

[7]. Li, Q., Zhao, X., Yang, J., 2015. Exploring the effects of nanocrystal facet orientations in g-C_3N_4/BiOCl heterostructures on photocatalytic performance. Nanoscale 7, 18971-18983.

[8]. Li, X., Wang, L., Lu, X., 2010. Preparation of silvermodified TiO_2 via microwave-assisted method and its photocatalytic activity for toluene degradation. J. Hazard Mater. 177, 639-647.

[9]. Liu, L.F., Barford, J., Yeung, K.L., 2007. Non-UV based germicidal activity of metal-doped TiO_2 coating on solid surfaces. J. Environ. Sci. 19, 745-750.

[10]. Mo, J., Zhang, Y., Xu, Q., Lamson, J.J., Zhao, R., 2009. Photocatalytic purification of volatile organic compounds in indoor air: a literature review. Atmos. Environ. 43, 2229-2246.

[11]. Spadavecchia, F., Ceotto, M., Presti, L. L., Aieta, C., Biraghi, I., Meroni, D., Ardizzone, S., Cappelletti, G. (2014). Second generation nitrogen doped titania nanoparticles: A comprehensive electronic and microstructural picture. Chin. J. Chem. 32, 1195-1213.

[12]. Doong, R. A., C. H. Chen, R. A. Maithreela, Chang, S. M. (2001). The Influence of pH and cadmium sulfide on the photocatalytic degradation of 2-Chlorophenol in titanium dioxide suspensions. Water Research 35, 2873-2880.

[13]. Adeleye, A.S., Stevenson, L.M., Su, Y., Nisbet, R.M., Zhang, Y., Keller, A.A., 2016. Influence of phytoplankton on fate and effects of modified zerovalent iron nanoparticles. Environ. Sci. Technol. 50, 5597-5605.

[14]. Massoudinejad, M., Mohseni, S.M., Ghaderpoori, M., Sarkhosh, M., Sahebi, S., 2019. Improvement of montmorillonite adsorption capacity for lead ions by modifying with hexadecyl trimethyl ammonium chloride: Characterization, modelling and optimization studies. Methods X 6, 2217-2219.

[15]. Cho, M., H. Chung, W. Choi, Yoon, J. (2004). Linear correlation between inactivation of *E. coli* and OH radical concentration in TiO_2photocatalytic disinfection. Water Research 38, 1069-1077.